# Spherical micromirrors from templated self-assembly: Polarization rotation on the micron scale

S. Coyle, G. V. Prakash, and J. J. Baumberg[a)]
*Department of Physics and Astronomy, University of Southampton, Southampton, SO17 1BJ, United Kingdom*

M. Abdelsalem and P. N. Bartlett
*Department of Chemistry, University of Southampton, Southampton, SO17 1BJ, United Kingdom*

(Received 14 February 2003; accepted 27 May 2003)

We demonstrate a fabrication route to individual micron-scale metallic spherical mirrors. The mirrors are prepared by electrochemical growth through the interstitial voids of a self-assembled latex sphere template. Excellent spherical mirrors of Au and Pt are obtained with unusual polarization properties in which multiple reflections with distinct anisotropies are found due to geometric polarization rotation. Such micromirrors can form the basis of low-cost microcavity structures and microlasers. © *2003 American Institute of Physics.* [DOI: 10.1063/1.1595723]

The ability to integrate micromirrors has tremendous technological potential, as shown by the Texas Instruments designed Digital Micromirror Device (Plano, TX).[1] However, despite the increasing use of microlens arrays in integrated optics, to our knowledge, no spherical negative-curvature micromirrors have been reported. In this letter, we demonstrate geometric reflections and polarization rotation of light from highly reflecting metallic spherical reflectors produced through low-cost electrochemical deposition and self-assembled templates.

Planar microcavities have been widely used as a way to control spontaneous emission and to enhance the interaction of light with matter, as in quantum wells (QWs)[2] or quantum dots,[3] but these structures only confine photons in one dimension. Confinement in lateral dimensions, such as in photonic crystals[4] or microcavity mesas,[5] can inhibit spontaneous emission altogether, but involves complex and expensive fabrication strategies. Here, we present a simpler approach utilizing spherical microcavities. While traditional lasers built from discrete components use macroscopic spherical mirrors, microcavity lasers do not. Nonplanar QW microcavity lasers have been fleetingly studied and can show low-threshold operation[6] but progress has been delayed by their fabrication problems. Theoretical work on the mode structure in parabolic dome[7] and spherical cavities[8] also highlight the promise of such zero-dimensional (0D) microcavities, but fabrication is nontrivial. Similarly, glass or polymer microspheres show high $Q$ factors in whispering gallery modes but it is generally hard to control them and difficult to couple light into and out of them.[9]

The use of metallic mirrors, rather than dielectric mirrors, in a spherical geometry simplifies fabrication. Although metallic mirrors exhibit relatively low $Q$ factors, the optical field penetrates far less in metallic microcavities than in dielectric ones, so significant and useful field enhancement is possible as shown in polymer-filled metallic planar microcavities.[10] Until recently, making curved mirrors in the size range required has been difficult, but advances in electrochemistry and directed self-assembly of colloidal templates now offer a cheap and simple way to produce an array of well-ordered spherical reflecting surfaces.[11] Previously, we have concentrated on making templates with latex spheres in the size range 200 nm–1 $\mu$m,[12] smaller than optimal for our microcavities. Here, we study the growth and reflection characteristics of single, and arrays of, spherical Pt and Au mirrors, of diameters, $\phi$, up to 10 $\mu$m.

The template is prepared through sedimentation of a confined colloidal solution of latex spheres on a gold-coated substrate electrode to leave a self-assembled arrangement. Either close-packed arrays or isolated sphere templates can be obtained by adjusting the sphere concentration. The substrate is then placed in an electrochemical cell with a solution of aqueous metal complex ions which are deposited through reduction in the interstitial spaces of the template [Fig. 1(a)]. The latex spheres are removed by dissolving in toluene, leaving a porous metallic ''cast'' with the ordering and size of the original template. The lack of strain in three-dimensional microstructures after this etching step (compared to fabrication using silica spheres) produces robust structures which have not shrunk. The electrochemical deposition is calibrated so that measurement of the total charge passed allows precise control of the film thickness. Scanning electron microscopy (SEM) micrographs are used to measure the pore mouth opening to check the thickness, $t$, of the film and investigate its surface quality, but do not give any indication of the quality of the surface of the cavities. The micrograph shown in Fig. 1(b) shows Au cavities of $\phi = 5$ $\mu$m and $t = 2$ $\mu$m, in a close-packed arrangement.

Structures greater than a micron in size are large enough to be studied in detail in a reflection microscope without diffraction artifacts. The geometric reflection paths of incident light on a curved reflector are shown in Fig. 1(c). The rays collected in the focal plane are those that leave the film near normally. Rays incident on other points of the surface either leave the film at large oblique angles such that they are not collected, or are collected but focused at a different focal plane.

[a)]Electronic mail: j.j.baumberg@soton.ac.uk

 

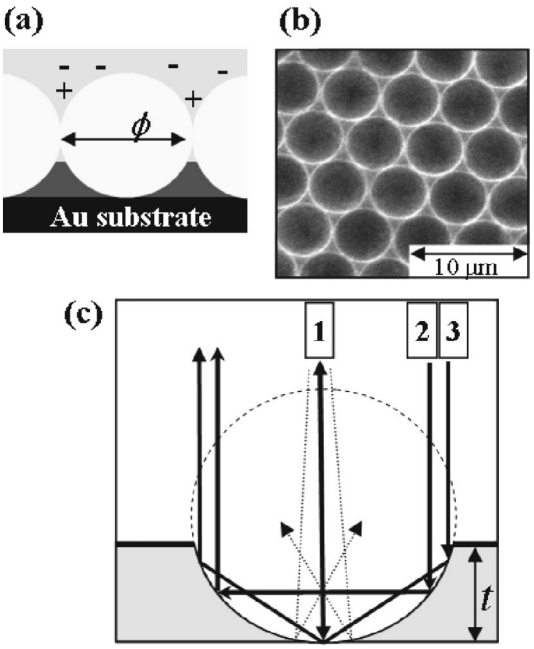


FIG. 1. (a) Schematic templating route uses electrochemical deposition in the interstitial holes of a self-organized template of latex spheres, up to a well-controllable height. (b) SEM of a Au microreflector with diameter $\phi = 5\ \mu$m, thickness $t = 2\ \mu$m. (c) Ray paths of reflections of an incident plane wave off the micromirror, full lines show collimated beams which are collected and dashed lines show near-axis paraxial rays which are focused inside the structure and defocused in collection.

Contact-mode atomic force microscopy (AFM) measurements of two films, the Au film ($\phi = 5\ \mu$m, $t = 2\ \mu$m) shown in Fig. 1(b) and a Pt film ($\phi = 10\ \mu$m, $t = 3\ \mu$m) reveal significant differences in their topography (Fig. 2) compared to the latex template (shown dashed). Cavities in the Au film [Fig. 2(a)] have a smooth spherical surface around their base and although the upper surface undulates, the surface around the latex sphere is smooth. In contrast, the surface of the Pt sample is much rougher [Fig. 2(b)] for the particular deposition conditions we employ—only the first 0.5 $\mu$m thickness of the film has a smooth spherical shape. Above this, the growth slows down except for points directly between the latex spheres, providing uneven surfaces. These observations are typical of the differences between microreflectors of Au and Pt across samples of many thousands of cavities. We find little effect in either the structure or the optical properties due to changes in the proximity between cavities, thus enabling a large variety of microcavity device designs. While the Au film can support double (and triple) bounces [Fig. 2(a), dotted line], the Pt mirrors only show single bounce reflections [Fig. 2(b)].

Optical images of the two samples are taken with $\times 200$ magnification, (numerical aperture $= 0.9$). Bright-field images of the Au cavities show that each cavity has a bright central spot seen in the center of a dark circle, which in turn is surrounded by a bright ring [Fig. 3(a)]. Further out, each cavity has six hexagonally arranged bright spots around it, which are Au pillars growing up through the triangular interstices between the latex spheres.[11,12] The top surface of the film is reflective, despite the mild irregularity seen in the AFM images (and are common in thick electrodeposited metal films). In contrast, bright-field images of the Pt sample [Fig. 3(b)] show the surrounding surface of the film is non-

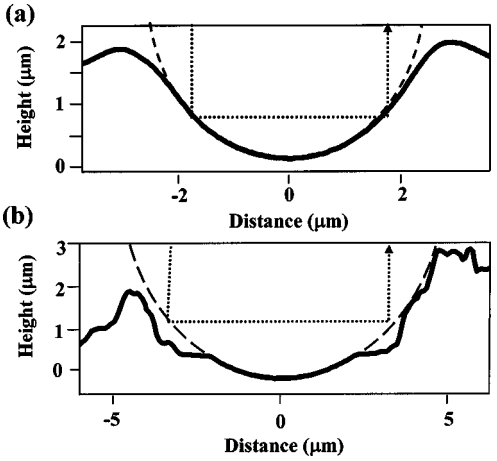


FIG. 2. Contact-mode AFM cross sections of (a) Au and (b) Pt films, across the center of a cavity. The outline of the latex sphere (dashed line) and the ray path of the two-bounce reflection (dotted line) are marked.

reflective, as suggested by the AFM scans. Dark-field images show background reflections of $< 1\%$ on the mirror surfaces confirming that their granular morphology acts to absorb the incident light. Thus, by adjusting the parameters for electrodeposition of different metals, it is possible to control whether the spherical microreflectors are embedded in reflecting or absorbing films, which is of considerable advantage for their application in microcavity devices since background reflection outside the microcavities can be suppressed.

The surrounding rings of high reflectivity observed arise from multiple bounces that are not normally seen from spherical reflectors due to their typically small curvature, $t/\phi \ll 1$. However, for the structures here $t \sim \phi/2$, and these multiple-bounce reflections are clearly present. By growing different thicknesses, the multiple bounces can be removed

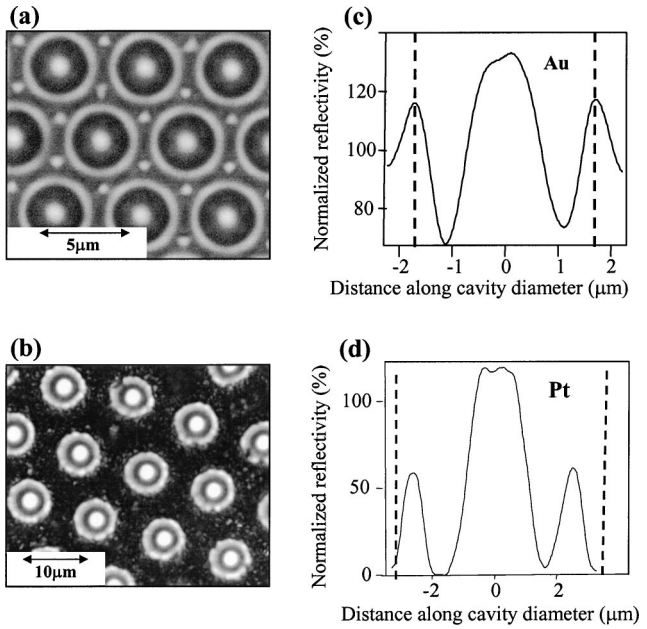


FIG. 3. (a, b) Bright-field images at $\times 200$ magnification of (a) diameter $\phi = 5\ \mu$m Au film and (b) $\phi = 10\ \mu$m Pt film. The top surface in (b) is nonreflective. (c, d) Cross sections of the reflectivity profiles of (c) Au and (d) Pt microreflectors (dashed lines indicate the theoretical positions of the double bounce).

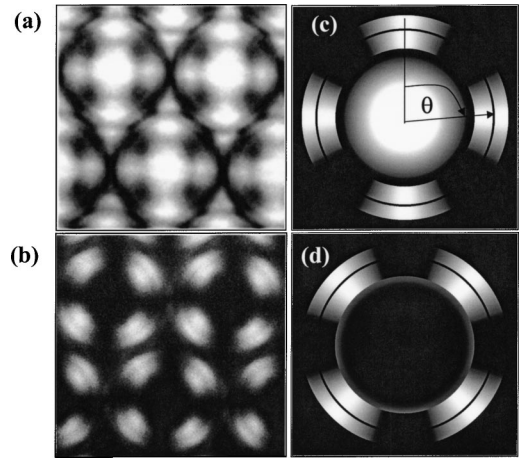


FIG. 4. Bright-field reflection images at ×200 magnification of Au microcavities for (a) collinear polarization and (b) cross linear polarization. (c) and (d) Predicted images of a cavity illuminated by plane waves, from geometric polarization rotation.

leaving only the central spot. Sections of the intensity profiles for each sample, normalized with respect to a planar silver mirror, are shown in Figs. 3(c) and 3(d). Both show a reflectivity greater than 100% at the center spot, demonstrating that light is indeed focused by the curved surfaces. Dashed lines in Fig. 3 indicate the predicted position of the double bounce from a cavity with a perfect spherical structure. Good agreement between theory and experiment is found for the Au sample, whereas the Pt sample shows a separate single-bounce reflection ring off the plateau region, which is confirmed by the AFM measurements. Thus, the optical quality of the metal surfaces can be directly confirmed, and used to optimize the electrochemical growth around the latex micromolds.

The validity of the ray model was further tested by analyzing the polarization state of the reflection from the micromirrors. Bright-field images of the Au sample are taken through collinear polarizers [Fig. 4(a)] and through crossed polarizers [Fig. 4(b)], with the incident polarization set to be vertical with respect to the images. Collinear polarizer alignment only images cavity reflections which preserve the polarization state, such as from the single reflection off the bottom of the cavity. Light experiencing a multiple reflection off the sides of the cavity acquires a more complicated polarization state depending on where on the sphere the light hits with respect to its polarization. In Fig. 4, the polarization state is preserved for light hitting the top, bottom, left- and right-hand sides of the microreflector. At other positions on the sides of the reflector (i.e., along the diagonal orientation), the polarization is rotated as seen in Fig. 4(b). In order to model this system, we denote the angle $\theta$ as the angle between the incident polarization and the point on the ring at which an incident ray hits. The origin of the polarization rotation is geometric—at each interface, the light picks up a twist in the linear polarization of $\theta$ due to the out-of-plane reflection geometry. Hence, for the double bounce, this polarization rotation is $2\theta$. The intensity distribution through collinear polarizers is therefore given by $I=\cos^2(2\theta)$. The predicted intensity distribution of the microcavity modeled for a copolarized or cross polarized analyzer [Figs. 4(c) and 4(d)] matches the results extremely well. As predicted, these polarization effects observed for Au are not present for the Pt samples which have no double bounce when grown in this way. These polarization anisotropies are thus a useful optical signature for large curvature micron-scale reflectors.

By capping these microcavity films with dielectric or metallic mirrors, 0D confined optical cavities can be produced with sharp resonant optical modes. In addition, they can be filled with a wide variety of optically active materials, including liquid crystals, semiconductors, chemical dyes, fluorescently tagged biomolecules, or semiconductor quantum dots. Further work is continuing to investigate how light couples to these reflectors with a view to making arrays of micron-sized lasers with ultralow lasing thresholds. In addition, they are promising for applications in integrated atom chips. The double-bounce reflection also offers the opportunity to make Raman oscillators by exciting whispering gallery modes in embedded dielectric microspheres.[13] The model described here can also be applied to much smaller cavities ($\phi=100$ nm to 950 nm) which cannot be so easily imaged optically, and do not give such a simple ray picture due to the comparable influence of diffraction.[14] However, the model discussed here is the first step in understanding the optical response of all such nanocavities.

In conclusion, we have demonstrated the reflection characteristics of electrochemically grown spherical microreflectors using a low-cost controllable self-assembled template. We explain their optical properties using a geometric model based on their actual morphology. Using such techniques, a wide range of microcavity designs can be implemented, because of the flexibility of this process.

The authors acknowledge support from the EU SQuID program, and EPSRC GR/N37261, GR/R54194, GR/S02662, and GR/N18598.

[1] http://www.dlp.com
[2] P. G. Savvidis, J. J. Baumberg, R. M. Stevenson, M. S. Skolnick, D. M. Whittaker, and J. S. Roberts, Phys. Rev. Lett. **84**, 1547 (2000).
[3] H. Saito, K. Nishi, I. Ogura, S. Sugou, and Y. Sugimoto, Appl. Phys. Lett. **69**, 3140 (1996).
[4] E. Yablonovitch, Phys. Rev. Lett. **58**, 2059 (1987).
[5] J. M. Gerard and B. Gayral, J. Lightwave Technol. **17**, 2089 (1999).
[6] F. M. Matinaga, A. Karlsson, S. Machida, Y. Yamamoto, T. Suzuki, Y. Kadota, and M. Ikeda, Appl. Phys. Lett. **62**, 443 (1993).
[7] J. Nockel, G. Bourdon, E. Le R. R. Adams, I. Robert, J.-M. Moisson, and I. Abram, Phys. Rev. E **62**, 8677 (2000).
[8] R. A. Abram, S. Brand, M. A. Kaliteevski, and V. V. Nikolaev, Phys. Status Solidi **183**, 183 (2001).
[9] R. Jia, D.-S. Jiang, P.-H. Tan, and B.-Q Sun, Appl. Phys. Lett. **79**, 153 (2001).
[10] P. A. Hobson, W. L. Barnes, D. G. Lidzey, G. A. Gehring, D. M. Whittaker, S. Skolnick, and S. Walker, Appl. Phys. Lett. **81**, 3519 (2002).
[11] P. N. Bartlett, P. R. Birkin, and M. A. Ghanem, Chem. Commun. (Cambridge) **2000**, 1671.
[12] M. C. Netti, S. Coyle, J. J. Baumberg, M. A. Ghanem, P. Birkin, and P. N. Bartlett, Adv. Mater. (Weinheim, Ger.) **13**, 1369 (2001).
[13] S. M. Spillane, T. J. Kippenberg, and K. J. Vahala, Nature (London) **415**, 621 (2002).
[14] P. N. Bartlett, J. J. Baumberg, S. Coyle, and M. Abdelsalam, Faraday Discuss., 125 (2003).